This is an electronic version of an article published in Philosophical Magazine Vol. 85, 2005, 1611–1623 (copyright Taylor & Francis). Philosophical Magazine is available online at:
http://journalsonline.tandf.co.uk/
http://www.informaworld.com/smpp/content content=a714032209 db=all order=page

Formal conditions for unambiguous residual strain determination by CBED

A.Morawiec

Polish Academy of Sciences, Institute of Metallurgy and Materials Science,
Reymonta 25, 30–059, Kraków, Poland
E–mail: nmmorawi@cyf-kr.edu.pl
Tel: (48) (12) 637-4200
Fax: (48) (12) 637-2192

Abstract

The method of residual strain determination using convergent beam electron diffraction (CBED) is attractive because of its good spatial resolution. However, attempts to obtain all six independent strain components from a CBED pattern lead to ambiguous results. The paper contains analysis of the ambiguities based on the complete algorithm for matching experimental and strain dependent simulated CBED patterns. The strain parameters which are not determinable by the CBED method are identified by examination of the most common goodness–of–fit functions. The indeterminable parameters are confirmed to be the '13' and '23' components and a combination of the diagonal components of the tensor given in the Cartesian system having the '3' axis parallel to the beam direction. The ambiguity can be eliminated based on multiple diffraction patterns. It is shown that two different patterns may be insufficient to get a unique strain tensor. The ambiguity can be removed only if certain characteristics of the two patterns are different, or if more than two patterns are used.

§1. Introduction

Elastic stresses that are locked into polycrystals influence properties of these materials. Sometimes, the effect of these residual stresses is beneficial, and sometimes it is harmful. Local stresses in microelectronic semiconductor devices lead to the formation of crystal defects and to degraded functioning. Application of surface layers induces residual stresses causing de-bonding or failure at interfaces. Heat treatment frequently leaves undesired high residual stresses in materials or parts, e.g. the quality of welded joints is influenced by stresses. The stress caused failure leads to scrapping products being well advanced in a manufacturing chain. Ultimately, the lack of understanding residual stresses has productivity and environmental implications. Understanding residual stresses plays a significant role in explaining and then preventing failure of components.

Determination of related residual strains is important for selecting optimal processing and service conditions. There are a number of methods of residual strain determination using x-ray diffraction, neutron diffraction, strain gauges, ultrasonic methods, micro-Raman spectroscopy; attempts are being made to use electron back-scattering diffraction. However, all of the above have poor spatial resolution comparing to the strain determination using transmission electron microscopy (TEM) and convergent beam electron diffraction (CBED) patterns. With the potential strain sensitivity of two parts per ten thousand and the spatial resolution of a few nanometers, CBED is the method of choice for all investigations of strains at the smallest scale, e.g. in microelectronic devices. And that occurs despite some stress relaxation due to sample thinning, which is the main negative aspect of the TEM strain measurements. Thanks to the spatial resolution, local strains can be correlated with microstructure elements and crystallite orientations. This makes the CBED method indispensable for investigating materials with properties influenced by microstructure or local crystallographic texture.

In recent years, numerous papers about CBED strain measurements have been published. In all cases, strain is determined numerically by minimisation of 'differences' between experimental and simulated patterns with respect to unit cell parameters or strain tensor components. Some of the early papers contain categorical statements claiming the possibility of definite strain determination. These claims turned out to

be unjustified. Although problems were indicated earlier (Humphreys 1991), the work of Maier *at al.* (1996) made it clear that a solution obtained from a CBED pattern cannot be unique because 'most CBED patterns can be simulated by a number of different lattice parameters'. The authors conclude by noting that 'a general recipe to the use of CBED patterns for evaluation of lattice parameters does not exist, since there are many parameters involved in the process.' They propose to approach the problem by an 'intelligent choice' of zone axes, and by making 'educated assumptions about the specimen'. Some numerical methods of eliminating the ambiguity were proposed (e.g. Rozeveld and Howe 1993). However, these approaches do not ascertain unique strain components (c.f. Wittmann *et al.* 1998, Wittmann *et al.* 2000). In these circumstances, the ambiguity problem is addressed by assumptions about the nature of strain, i.e. by limiting the number of variable parameters. Even if such assumptions are justified, in the presence of experimental errors, serious difficulties appear in the form of instabilities of the final results. This hinders the development of fully functional systems for strain determination.

The main subject of this paper is the separation of determinable strain components from those which cannot be reliably evaluated. Contrary to the common opinion (c.f. Maier *at al.* 1996), the large number of variable parameters is not the main source of the ambiguity problem; even with a limited number of variables, one may face ambiguous solutions. The problem is caused by the measurement geometry, which leads to 'inconvenient' goodness-of-fit functions. It follows from this geometry that the ambiguity issue becomes more transparent when tensor quantities are expressed in the microscope coordinate system because the sensitivity to displacements in the plane perpendicular to the beam direction must be higher than to displacements parallel to that direction. We confirm that in the presence of experimental errors, the standard CBED based method cannot resolve values of certain parameters which can be expressed as simple combinations of the strain components given in the microscope coordinate system. The essential contributions of this paper are the explicit expression of the the goodness–of–fit as a function of strain and clear identification of the indeterminable parameters in the cases of one and multiple patterns used in the strain measurement. By focusing on the complete strain tensor, the paper provides firm ground for confronting legitimate assumptions an experimenter may take (e.g. incompressibility, plain stress et cetera)

with the capability of the method to determine the paramaters not restricted by these assumptions. Understanding the ambiguity problem will create a stable foundation for the 'intelligent choice' and 'educated assumptions' proposed by Maier *at al.* (1996).

Despite the importance of the indeterminable parameters for the CBED method, previous accounts on the subject are cursory and conflicting. Questions about the dimensionality of the manifold of indeterminable parameters were asked by Wittmann *at al.* (2000). Among various approaches to resolve the issue, these of Toda *et al.* (2000) and Krämer *et al.* (2000) are closest to our way of thinking. Both groups recognise the importance of specifying parameters in the microscope coordinate system. Toda *et al.* (2000) assume plane strain with three determinable parameters. Also three but different parameters are considered to be determinable by Krämer *et al.* (2000), and these results, for the most part, are confirmed in this paper.

All strain components can be reliably determined based on multiple patterns with different zone axes. The idea of using multiple tilts and voltages is quite trivial and has been mentioned before but it has not been really explored. We give general guidelines for approaching computational aspects of such method. It turns out that with standard experimental approach, two different zone axes may be insufficient to remove the ambiguity completely. Unique strain can be obtained only if certain numbers characterising the patterns have different values, or if three (or more) patterns are used.

Let us close this introduction with a note on our simplifying assumptions. First, our considerations are based on the geometric theory of diffraction (Ewald 1969). Having a thorough understanding of this simple case, one can proceed further with the refinement based on more adequate approaches because conclusions of this paper are applicable to procedures utilising dynamic corrections. Moreover, coordinate systems are assumed to be Cartesian; this does not apply to Appendix, where a more general system is used. Finally, the CBED based method is portrayed as a fine-tuning of six independent unit cell parameters but in reality the problem is more complex. Besides the unit cell parameters, also the effective voltage, the camera length and the misorientation between the reference model without strain and the investigated specimen must be attuned. Usually, most of these additional parameters are estimated beforehand based on factors not involving strain. Alternatively, schemes with more than six independent optimisation variables can be devised. However, these issues are not considered here.

§2. Geometry of HOLZ lines

As was already mentioned, in the CBED method, strain is determined by comparing experimental patterns with theoretically predicted models. In principle, the unknown parameters could be determined by fitting experimental and theoretical intensities (c.f. Zuo and Spence 1991). However, such an ideal approach is awkward. In practice, strain is calculated by fitting characteristic geometric elements of high order Laue zone (HOLZ) line patterns; in particular, distances between intersections of the lines are matched. The calculation is based on equations for the locations of the intersection points and their dependence on strain. Since we have not encountered a complete formulation of this dependence in literature, appropriate relationships are given below.

Let b^i, $(i = 1, 2, 3)$ be the basis vectors of the crystal reciprocal lattice, and let λ be the radiation wavelength. Within the geometric theory, the wave vectors k_0 and k of the incident and reflected beams, respectively, are governed by the Laue equation $k - k_0 = g$, where $k \cdot k = 1/\lambda^2 = k_0 \cdot k_0$, and g is a reciprocal lattice vector, i.e. $g = \sum_{i=1}^{3} h_i b^i$, and h_i are integer Miller indices. In the convergent beam technique, the incident beam direction k_0 is variable. Elimination of k_0 from the Laue equation and the relation $k \cdot k = k_0 \cdot k_0$ leads to the well known relationship

$$2g \cdot k = g \cdot g \ . \tag{1}$$

With fixed g, this equation describes a circle on the sphere $k \cdot k = 1/\lambda^2$. The circle determines a (Kossel) cone visible on a microscope viewing screen as a so–called K–line, which in the considered circumstances is a HOLZ line. Eq.(1) is the basis for the elementary description of the geometry of K–line patterns (see, e.g. Cowley 1981).

A homogeneous displacement represented by a 3×3 matrix F transforms direct space vectors according to $x' = Fx$. The displacement involves both rotation and stretch; they are factors in the polar decomposition $F = RU$, where R is an orthogonal matrix representing the rotation, and a symmetric positive definite matrix U represents the stretch. The resulting finite Lagrangian strain is given by $(F^T F - I)/2$, were I is the identity matrix. Since only small displacements are considered, strain can be expressed as $\varepsilon \approx (F + F^T)/2 - I \approx U - I$. In this case, F is 'close' to I, and $H := (F^T)^{-1}$ is well defined. The displacement represented by F transforms the basis vectors b^i to $b^{i'} = Hb^i$. Hence, the rule for the transformation of a general reciprocal lattice vector

is

$$g' = \sum_{i=1}^{3} h_i b^{i'} = Hg \ . \tag{2}$$

Based on (1), the equations

$$2g'_1 \cdot k' = g'_1 \cdot g'_1 \ , \quad 2g'_2 \cdot k' = g'_2 \cdot g'_2 \quad \text{and} \quad k' \cdot k' = 1/\lambda^2 \tag{3}$$

corresponding to reflections $g'_1 = Hg_1$ and $g'_2 = Hg_2$ determine the wave vector k' of the intersection of two HOLZ lines in a pattern originating from a crystallite transformed by F. The solution of the system (3) is given in the Appendix. It has the property

$$k' = \kappa(Hg_i, I) = H\kappa(g_i, H^T H) \qquad (i = 1, 2) \ , \tag{4}$$

where the second argument of κ is related to the crystallographic metric. The relationship (4) emphasises the form of the dependence of k' on strain and the rotational part of the displacement: only $H^T H$ in (4) depends just on strain, while the factor H $(= RU^{-1})$ contains both strain and rotational components. In relation to the considered pattern matching, the orientation of a sample generating an experimental pattern is never exactly the same as the orientation used in a simulation, and this misorientation is manifested by a non–trivial R. Ideally, to eliminate this effect, the goodness–of–fit should be independent of the sample orientation. This means that the goal function should be based on the R–independent scalar products $k'_{(i)} \cdot k'_{(j)}$ and $k^{exp}_{(i)} \cdot k^{exp}_{(j)}$, where $k'_{(i)}$ are strain dependent vectors expressed by (4), $k^{exp}_{(i)}$ are vectors to points on the experimental patterns, and lower indices numerate the intersection points. Otherwise, the function involves the misorientation and the number of unknowns is increased by three independent misorientation parameters. In practice, the functions are selected in such a way that the dependence is weak, and it is assumed to be of no consequence. This approach is followed below. With the assumption that R equals I, we have $H = U^{-1} = (I + \varepsilon)^{-1} = I - \varepsilon$.

§3. Goodness–of–fit and its sensitivity to strain

The crystallographic calculations of the previous section are conveniently performed in a crystal coordinate system, whereas the data originating from TEM are given in the

microscope coordinate system. With O being the matrix representing the crystal orientation, the transformation H in the microscope coordinate system is $H^s = O^{-1}HO$, and the wave vector in the microscope coordinate system has the form $k'^s = O^{-1}k'$.

The experimental data are collected from a flat detector. A vector $v^s = [v_1^s\ v_2^s\ v_3^s]^T$ given in the microscope coordinate system with the '3' axis along the beam is projected on the detector as the two–dimensional vector $\mathcal{P}(v^s) = (L/v_3^s)[v_1^s\ v_2^s]^T$, where L is the effective camera length. The goodness–of–fit functions are defined based on locations of the HOLZ line intersection points for the experimental pattern and those for $\mathcal{P}(k'^s)$ which involve strain. The most common method is to match distances between the intersections. The theoretical distance d' between intersection points (i) and (j) is

$$d' = \mid \mathcal{P}(k'^s_{(i)}) - \mathcal{P}(k'^s_{(j)}) \mid \ . \tag{5}$$

A simple goodness-of–fit function may have the form

$$\psi \propto \sum_n (d'_{(n)} - c d^{exp}_{(n)})^2 \ , \tag{6}$$

where n numerates the measured distances $d^{exp}_{(n)}$, $d'_{(n)}$ is given by (5), and c is a variable magnification factor for fine-tuning L; see (Zuo 1992) and (Krämer *et al.* 2000). The magnification factor can be eliminated by fitting distance ratios; e.g. instead of (6), one can minimize $\sum_{m,n}(d'_{(m)}/d'_{(n)} - d^{exp}_{(m)}/d^{exp}_{(n)})^2$. In another method, areas of triangles defined by intersecting HOLZ lines are matched (Rozeveld *et al.* 1992).[1] In all these cases, the goodness–of–fit function is constructed using the projection $\mathcal{P}(k'^s)$ to determine d', and it depends on strain ε via

$$k'^s = O^{-1}\kappa((I - \varepsilon)g_i, I) \ .$$

The algorithm for the calculation of the function values is only slightly modified when the effective voltage approximation or individual shifts of HOLZ lines are used to take account of dynamic effects.

It is clear from this definition of the goodness–of–fit as a function of strain that the considered minimisation problem is well–posed (i.e. it has a unique solution depending continuously on the parameters). Using the above formulae, an explicit form

[1] This choice is based on the assumption that the areas of polygons are less sensitive to errors caused by dynamic effects at the intersections of HOLZ lines. That argument is questionable because both the distances and the areas are based on line locations, and the triangle areas are directly related to the distances (via Heron's formula).

of the function can be constructed. Unfortunately, because of the intricacy of κ, that expression is complicated even in simplest cases. (Linear approximations of the function are also involved.) However, properties of that function can be relatively easily investigated using computer assisted symbolic calculations. We have checked numerous patterns (zone axes [331], [230], [125], [334]), voltages (90, 120, 200kV) and goodness–of–fit functions (ψ, ratios of distances, triangle areas, ratios of triangle areas). Here, the analysis is illustrated by only one case (see Fig. 1) but the conclusions are general. *Fig. 1* The HOLZ lines and intersection points employed are shown in Fig. 2, and the indices *Fig. 2* of the lines are listed in Tab.1; cf. Krämer *et al.* 2000. *Tab. 1*

It is frequently underlined that due to the presence of HOLZ lines, the CBED patterns carry 'three dimensional information'. However, the region of the reciprocal space from which that data comes is still relatively flat; see Fig. 3. It is spread around *Fig. 3* the plane perpendicular to the microscope axis. Therefore, in terms of the sensitivity to strain, this particular direction is different than the directions perpendicular to it. Hence, it is rightful to expect that the issue will become clearer when the patterns are simulated for various components of the strain tensor ε^s ($= O^{-1}\varepsilon O$) given in the microscope coordinate system with one of its axes along the microscope axis. In fact, it shown below the sensitivity of patterns' geometry to different combinations of ε^s_{ij} varies drastically. This allows for a dichotomous division of parameters; those with negligible influence (smaller than the impact caused by random experimental errors) are refered to as indeterminable.

Since small (linear) strains are additive, an arbitrary strain can be represented as a composition of *elemental* strains with *one* non–vanishing ε^s_{ij} and other strain components fixed at zero. Due to the suitable choice of the coordinate system, some of the elemental strains can be identified as indeterminable. Analysis performed for all strain components shows that the dependence on ε^s_{11}, ε^s_{22}, ε^s_{33} and ε^s_{12} is much stronger than the dependence on ε^s_{13} and ε^s_{23}. For the considered example pattern, this is reflected by the table

$$\begin{bmatrix} 1.585 & 2.180 & 1.817\times10^{-4} \\ & 1 & 4.036\times10^{-4} \\ & & 0.968 \end{bmatrix},$$

with the entry ij equal to the ratio ψ_{ij}/ψ_{22}, where ψ_{ij} is the value of ψ for ε^s such that

$\varepsilon^s_{ij} = 0.001$ and all other independent entries are zero. (All distances between points marked in Fig. 2 were used, and c was fixed at 1.) In the case of non–zero ε^s_{12}, the strain caused shifts of the intersection points are relatively small but occur in different directions. On the other hand, large shifts caused by non–zero ε^s_{13} are parallel (Fig. 4); *Fig. 4* the strain with only ε^s_{23} being non–zero leads to a similar effect. Generally, the strains which are combinations of only ε^s_{13} and ε^s_{23} components cause changes observable as parallel shifts of the patterns. Since this effect cannot be distinguished from a rotation of the sample, such strains have little influence on the mutual distances between the intersection points and, consequently, on the goodness–of–fit. Fig. 5a illustrates the *Fig. 5* typical dependence of ψ on strain with varying determinable ε^s_{12} and indeterminable ε^s_{13} and other independent components equal to zero.

The strains ε^s_{13} and ε^s_{23} are the only indeterminable elemental strains but they do not exhaust the list of indeterminable parameters. Other indeterminable parameters can be linear combinations of ε^s_{11}, ε^s_{22}, ε^s_{33} and ε^s_{12}. Due to the axial symmetry of the measurement (with particular choice of HOLZ lines disregarded), the combinations must be symmetric with respect to indices 1 and 2. The most general strain of this kind is based on $\varepsilon^s_{11} = \varepsilon^s_{22}$, ε^s_{12} and ε^s_{33}. Analysis of the goodness–of–fit functions shows that there is one such indeterminable parameter, and it does not involve ε^s_{12}. Only the strain of the form

$$\operatorname{diag}(\varepsilon^s_{11}, \varepsilon^s_{11}, \varepsilon^s_{33}) =: e \operatorname{diag}(1, 1, \alpha) \tag{7}$$

with a fixed α and variable e has no influence on the pattern. (See Figs. 4c and 5b.) The observation confirms the comment made by Krämer *et al.* (2000), that the isotropic strain in the plane perpendicular to the beam has the same impact on a pattern as some extension along the beam. The coefficient α is close to 2 for common experimental conditions. Its precise value depends on magnitudes of reciprocal lattice vectors and the magnitude of the wave vector. (For the considered example, α turns out to be ~ 2.014 and its value decreases with voltage at the rate of about 0.004 per 1kV.) Since the dependence of α on strain is very weak, a good approximation can be calculated numerically for given voltage and zone axis. Assuming that α is known, the number of indeterminable parameters is three. By altering the part of strain described by (7), the trace of the tensor is modified, which means that the volumetric changes in the material are indeterminable. With $\alpha \neq 1$, the deviatoric part of is also affected.

The weak dependence of pattern geometry on ε^s_{13} and ε^s_{23} and $\varepsilon^s \propto \mathrm{diag}(1,1,\alpha)$ is a general rule. It occurs for other zone axes and voltages, and for other goodness–of–fit functions. In the presence of experimental errors, the minimisation problem becomes ill-conditioned (i.e. relative change in solution can be disproportionate to change in input data). The resulting ambiguity can be concisely characterised by the following statement: with δ_i $(i = 1, 2, 3)$ of the same order of magnitude as entries of ε^s, the shifts of intersection points caused by two different strains

$$\varepsilon^s \quad \text{and} \quad \varepsilon^s + \begin{bmatrix} \delta_3 & 0 & \delta_1 \\ 0 & \delta_3 & \delta_2 \\ \delta_1 & \delta_2 & \alpha\,\delta_3 \end{bmatrix}$$

are indistinguishable.

Based on the flatness of the detectable part of the reciprocal space, the intuitive guess could be that only plane strain is reliably determinable (see, e.g. Toda *et al.* 2000). However, this guess is inaccurate. In a sense, the CBED method is capable of providing more than just plane strain but on the other hand, a combination of ε^s_{ii} $(i = 1, 2, 3)$ components is indeterminable.

Krämer *et al.* (2000) indicate that two diffraction patterns can be used to get around the problem. But are two different patterns really sufficient? Let us assume that two data sets (ε^{s_1} and ε^{s_2}) for two zone axes (two orientations O_1 and O_2) are given. The relationships between the strain tensor ε in the crystal coordinate system and ε^{s_1} and ε^{s_2} given in the laboratory coordinate system are $O_1^{-1}\varepsilon O_1 = \varepsilon^{s_1}$ and $O_2^{-1}\varepsilon O_2 = \varepsilon^{s_2}$. With $\varepsilon^{s_j}_{13}$ and $\varepsilon^{s_j}_{23}$ $(j = 1, 2)$ considered to be unreliable and relations involving them disregarded, one has a system of eight linear equations

$$O_j^{-1}\varepsilon O_j - e_j\,\mathrm{diag}(1, 1, \alpha_j) = \varepsilon^{s_j} \tag{8}$$

for eight unknowns – six independent entries of ε and e_1 and e_2. (Subscripts are added to e and α to distinguish between quantities corresponding to different patterns.) For getting a unique strain from the two patterns, it is necessary that the system has a unique solution. However, the determinant of the system's matrix is proportional to $\alpha_1 - \alpha_2$. If $\alpha_1 = \alpha = \alpha_2$, the rank of the matrix equals seven[2], and there is one

[2]Except some special cases in which the rank can be lower, e.g. when the orientations differ by a rotation about the microscope axis.

indeterminable parameter, say δ, extended along the null space of the matrix. It can be verified by substitution into (8) that the null space is given by

$$\varepsilon = \delta \; O_1 N O_1^{-1} \quad \text{and} \quad e_1 = \delta = e_2 \; ,$$

where

$$N = \begin{bmatrix} 1 & 0 & \beta_1 \\ 0 & 1 & \beta_2 \\ \beta_1 & \beta_2 & \alpha \end{bmatrix} \; , \qquad \beta_i = \frac{(\alpha - 1)\Delta_{i3}}{2\Delta_{33}} \; , \qquad \Delta = O_1^{-1} O_2 \; ,$$

and, for simplicity, Δ_{33} is assumed to be non–zero. In other words, two different strains ε and $\varepsilon + \delta \, O_1 N O_1^{-1}$ lead to indistinguishable changes in geometry of the pairs of patterns. In practical situations with the same voltage and similar magnitudes of reciprocal lattice vectors, α_1 and α_2 may be very close, and two such patterns would not be sufficient for determining the complete strain; i.e. the application of two zone axes may only partially resolve the ambiguity issue. In order to get an unambiguous solution, experimental conditions must be selected in such a way that the difference between the α_j coefficients has a significant value.

Assuming equality of all α_j, there is a question whether the problem can be corrected by using more than two different beam directions. With special cases disregarded, the matrix of coefficients of the system has the rank equal to the number of unknowns. Thus, formally, to resolve the problem of ambiguities in the CBED strain determination, three or more patterns originating from the same area of the sample are sufficient. Using multiple zone axes means sacrificing spatial resolution but the latter will still remain high comparing to other strain determination techniques. It is recommended by Maier *et al.* (1996) that in order to retain the resolution, the tilt 'should be kept to a minimum'. This is in conflict with the objective of removing the ambiguity, since for the problem to be better conditioned, the tilt must be significant.

From the formal viewpoint, one possible way of determining all six independent strain components from multiple (three or more) patterns is by applying the standard approach to each of the patterns with ε^{s_j} as optimisation parameters; since $\varepsilon_{13}^{s_j}$, $\varepsilon_{23}^{s_j}$ and e_j have little influence on the goodness–of–fit, they can be initially set at zero. The next step is to use (8) ($j = 1, ..., J \geq 3$) to get the complete strain tensor in the crystal coordinate system. Knowing the latter, one can calculate the lattice parameters or strain tensor in other coordinate systems; this includes the possibility of calculating

$\varepsilon_{13}^{s_j}$, $\varepsilon_{23}^{s_j}$ and e_j. The results can be refined by repeating the procedure with the new values of $\varepsilon_{13}^{s_j}$, $\varepsilon_{23}^{s_j}$ and e_j at the optimisation step.

More elegant and simple method is to determine the complete strain by modifying the goodness–of–fit function so it concurrently involves data from multiple patterns. In the case of ψ (and the other functions mentioned above) the modification is simple: the sum must be extended over all the patterns. As in the previous approach, the crystal orientations O_j must be known beforehand.

§4. Conclusions

Explicit formulae for the locations of HOLZ line intersection points and a complete algorithm for the construction of the goodness–of–fit between simulated patterns allowed for quantitative analysis of the level of sensitivity of the goodness–of–fit functions to strain. The analysis shows that the problem of strain determination from one diffraction pattern is well–posed but ill–conditioned. Three independent strain components are indeterminable; these are the '13' and '23' entries and the part $e\,\mathrm{diag}(1,1,\alpha)$ of the tensor given in the coordinate system with the '3' axis being parallel to the beam direction. If parameters used in the optimisation process (e.g. unit cell parameters) effectively depend on any of these three components, they are unreliable.

Knowing the nature of ambiguities, one can make the CBED method more robust. The reliability of the results can be improved by using multiple zone axes. Each pattern provides three reliable strain components. These contributions are consistent in the sense that they originate from one strain state; they can be seen as different projections of the same entity. However, two different zone axes may be insufficient for unambiguous determination of the complete strain. In the standard experimental approach with patterns obtained at the same voltage, the characteristics α_1 and α_2 have similar values, and there is still one parameter with negligible influence on the goodness–of–fit. From the formal viewpoint, unique strain tensor can be obtained only if these characteristics are sufficiently different or if more than two different zone axes are used.

Acknowledgements

The author would like to thank Dr. E.Bouzy (Université de Metz) for the pattern shown in Fig. 1.

References

Cowley, J.M., 1981, *Diffraction Physics* (Amsterdam:North-Holland).

Ewald, P.P., 1969, *Acta Cryst. A* **25,** 103.

Humphreys, C.J., 1991, *Proceedings of the 9th International Conference Strength of Metals and Alloys,* edited by D.G.Brandon, R.Chaim and A.Rosen (London: Freund), pp.127-137.

Krämer, S., Mayer, J., Witt, C., Weickenmeier, A., and Rühle, M., 2000, *Ultramicroscopy* **81,** 245.

Maier, H.J., Keller, R.R., Renner, H., Mughrabi, H., and Preston, A., 1996, *Philos. Mag. A* **74,** 23.

Rozeveld, S.J., Howe, J.M., and Schmauder, S., 1992, *Acta Metall. Mater.* **40,** S173.

Rozeveld, S.J., and Howe, J.M., 1993, *Ultramicroscopy* **50**, 41.

Toda, A., Ikarashi, N., and Ono, H., 2000, *J. Cryst. Growth* **210,** 341.

Wittmann, R., Parzinger, C., and Gerthsen, D., 1998, *Ultramicroscopy* **70,** 145.

Wittmann, R., Kruse, P., Frauenkron, M., Gerthsen, D., 2000, *Philos. Mag. A* **80,** 2215.

Zuo, J.M., and Spence, J.C.H., 1991, *Ultramicroscopy* **35,** 185.

Zuo, J.M., 1992, *Ultramicroscopy* **41,** 211.

Appendix

It can be verified by substitution that equations

$$2g_i \cdot k = g_i \cdot g_i \quad (i = 1, 2) \quad , \quad k \cdot k = 1/\lambda^2 \tag{9}$$

are satisfied by

$$k = \frac{y \times z \pm y\sqrt{4y \cdot y/\lambda^2 - z \cdot z}}{2y \cdot y} \ , \tag{10}$$

where $y = g_1 \times g_2$ and $z = g_1(g_2 \cdot g_2) - g_2(g_1 \cdot g_1)$. If M is a matrix representing the metric in the reciprocal space, eqs.(9) can be written as

$$2g_i^T M k = g_i^T M g_i \quad (i = 1, 2) \quad , \quad k^T M k = 1/\lambda^2 \ . \tag{11}$$

The solution (10) takes the form

$$k = \kappa(g_i, M) = \frac{y \times (Mz) + \sqrt{\det(M)}\ \left(M^{-1}y\right)\ \sqrt{4\ \det(M)\,(y^T M^{-1} y)/\lambda^2 - z^T M z}}{2\ \det(M)\,(y^T M^{-1} y)} \ ,$$

where $y = g_1 \times g_2$, $z = g_1\,(g_2^T M g_2) - g_2\,(g_1^T M g_1)$, and $\times$ has only its algebraic meaning.

Now, let the vectors g_i be replaced by $g_i' = Hg_i$; cf. eq.(2). Equations $2g_i' \cdot k' = g_i' \cdot g_i'$ and $k' \cdot k' = 1/\lambda^2$ are solved by

$$k' = \kappa(Hg_i, M) \ .$$

On the other hand, these equations can also be expressed as $2g_i^T A l' = g_i^T A g_i$ and $l'^T A l' = 1/\lambda^2$, where $l' = H^{-1}k'$ and $A = H^T M H$. In this form, they are identical to eqs.(11). Hence, $l' = \kappa(g_i, A)$ or

$$k' = H\kappa(g_i, H^T M H) \ .$$

With $M = I$, one gets eq.(4).

Captions

Figure 1. The [331] diffraction pattern of Si obtained for 119.2kV. Geometry of this pattern is used as an example throughout the paper.

Figure 2. Schematic of the pattern shown in Fig. 1. Cubic lattice with the constant of $a = 0.54307$nm was used to simulate the pattern.

Figure 3. Projection of the reciprocal lattice nodes listed in Tab.1 on the plane perpendicular to the $[\overline{1}\ \overline{1}\ 6]$ direction. The nodes are marked by disks. For reference, the locations of (3 3 1) and $(\overline{5}\ 5\ 0)$ are marked as squares.

Figure 4. The shift of the intersection points (dots) for the strain with $\varepsilon^s_{12} = 0.001$ (a), $\varepsilon^s_{13} = 0.001$ (b) and $\varepsilon^s = 0.001 \times \mathrm{diag}(1, 1, 2)$ (c). The other independent strain components are zero. For reference, the locations of the points corresponding to the material without strain are marked by crosses.

Figure 5. (a) The dependence of ψ on ε^s_{12} (horizontal axis) and ε^s_{13} (vertical axis). The other strain components are zero. The values of isolines are omitted for clarity; to make the point, it is sufficient to indicate that the ratio between the values at $(\varepsilon^s_{12} = 0.001, \varepsilon^s_{13} = 0)$ and $(\varepsilon^s_{12} = 0, \varepsilon^s_{13} = 0.001)$ is $\sim 1.2 \times 10^4$. (b) The dependence of ψ on ε^s_{33} (horizontal axis) and $2\varepsilon^s_{11}$ (vertical axis), for the strain tensor given by $\varepsilon^s = \mathrm{diag}(\varepsilon^s_{11}, \varepsilon^s_{11}, \varepsilon^s_{33})$. The ratio between the values at $2\varepsilon^s_{11} = 0.001 = -\varepsilon^s_{33}$ and $2\varepsilon^s_{11} = 0.001 = \varepsilon^s_{33}$ is $\sim 2.0 \times 10^4$.

Table 1. Miller indices of the HOLZ lines shown in Fig. 1.

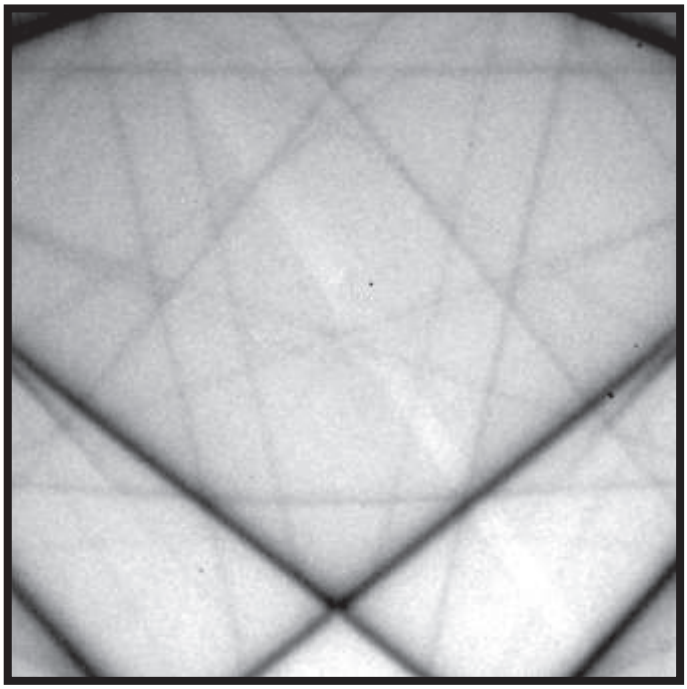

Figure 1.

A.Morawiec, *... residual strain determination ...*

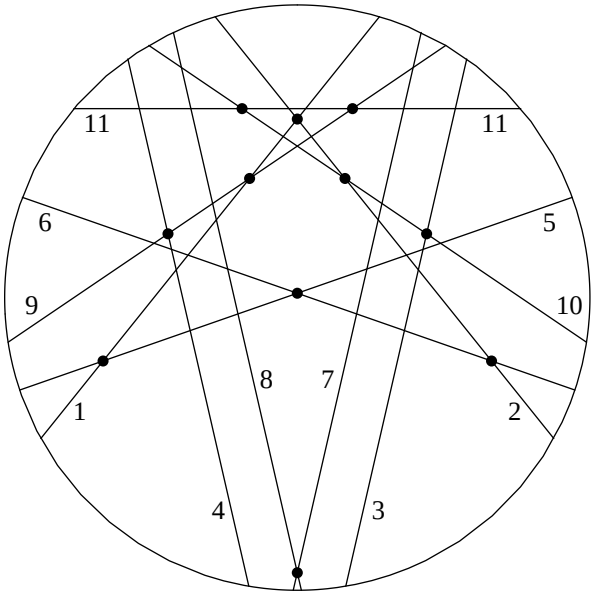

Figure 2.

A.Morawiec, *... residual strain determination ...*

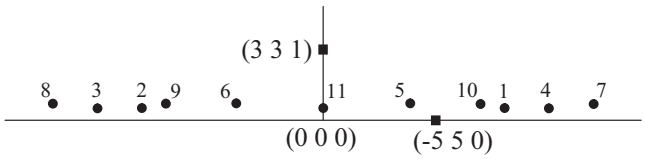

Figure 3.

A.Morawiec, *... residual strain determination ...*

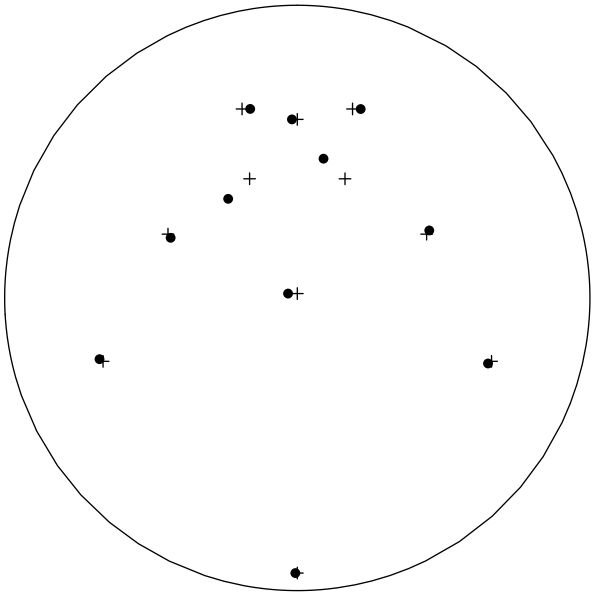

Figure 4a.

A.Morawiec, *... residual strain determination ...*

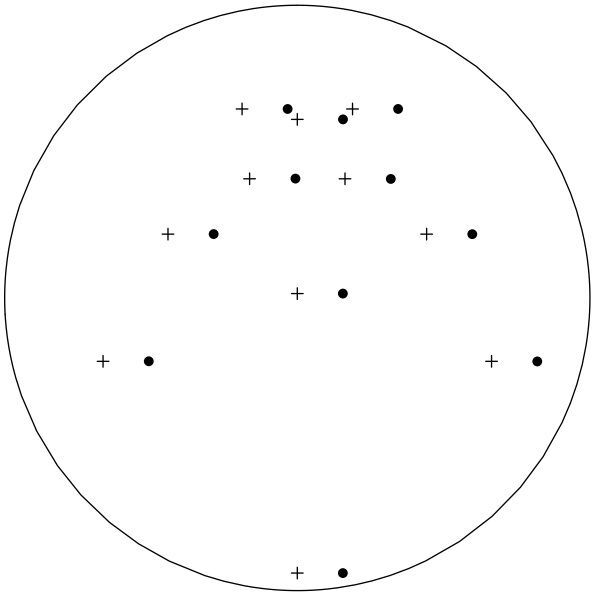

Figure 4b.

A.Morawiec, *... residual strain determination ...*

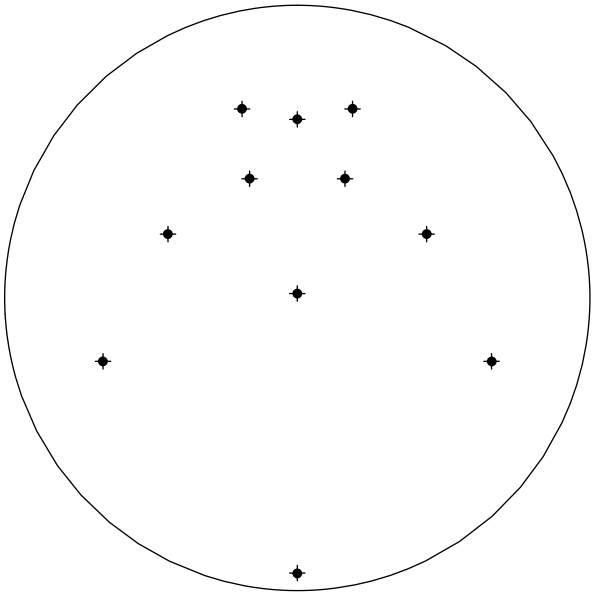

Figure 4c.

A.Morawiec, *... residual strain determination ...*

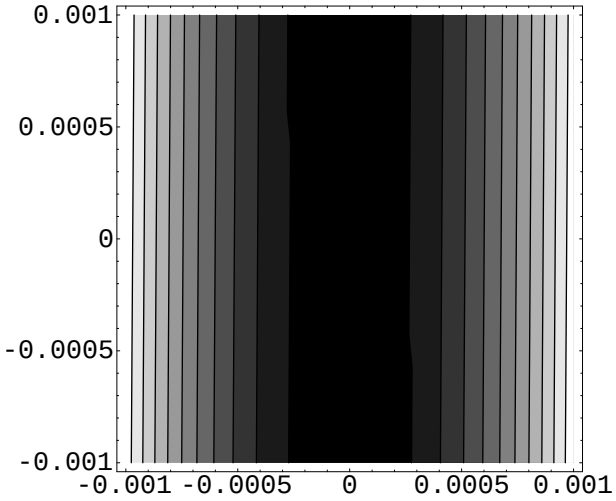

Figure 5a.

A.Morawiec, *... residual strain determination ...*

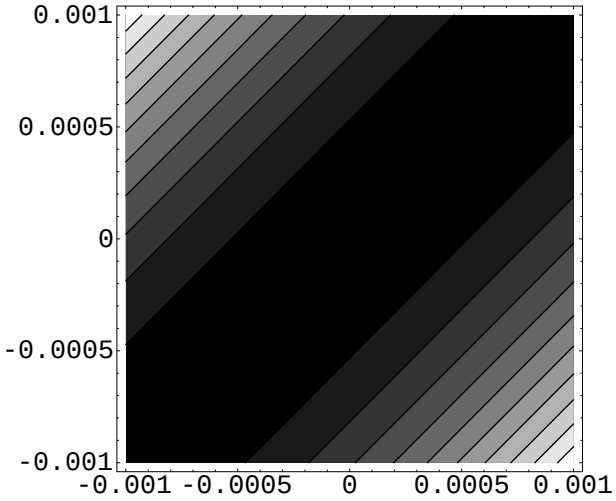

Figure 5b.

A.Morawiec, *... residual strain determination ...*

1	$(\overline{9}\ 7\ 9)$	5	$(\overline{6}\ 2\ 16)$	9	$(10\ \overline{4}\ \overline{14})$
2	$(7\ \overline{9}\ 9)$	6	$(2\ \overline{6}\ 16)$	10	$(\overline{4}\ 10\ \overline{14})$
3	$(11\ \overline{9}\ \overline{3})$	7	$(\overline{12}\ 12\ 4)$	11	$(3\ 3\ \overline{15})$
4	$(\overline{9}\ 11\ \overline{3})$	8	$(12\ \overline{12}\ 4)$		

Table 1.